Bead-to-Fiber Transition in Electrospun Polystyrene

Goki Eda, Satya Shivkumar

Department of Mechanical Engineering, Worcester Polytechnic Institute, Worcester, Massachusetts 01609

Received 16 May 2006; accepted 26 November 2006
DOI 10.1002/app.25907
Published online 26 June 2007 in Wiley InterScience (www.interscience.wiley.com).

ABSTRACT: The morphological transition, namely bead-to-fiber transition, of electrospun polymer was examined for polystyrene, with its molecular weight ranging from 19,300 to 1,877,000 g/mol. Tetrahydrofuran and *N*,*N*-dimethylformamide were used as solvents to examine the effects of solvent properties on the morphological variations. Polymer molecular weight and solvent properties had a significant effect on the morphology of beads as well as fibers. Observation of fiber diameter and its distribution suggested that the effect of molecular weight and solvent may be independent. The critical concentrations at which incipient and complete fibers were observed were found to decrease significantly with molecular weight, as can be expected. The effect of solvents on these critical concentrations was minimal for moderate to high-molecular-weight (>100,000 g/mol) solutions. For low-molecular-weight solutions, the transition occurred at concentrations much lower than those predicted by a model, based exclusively on chain entanglements. Rapid solidification of jet which is expected to occur with concentrated solutions may play a vital role in establishing stable fibers during electrospinning. © 2007 Wiley Periodicals, Inc. J Appl Polym Sci 106: 475–487, 2007

Key words: electrospinning; polystyrene; molecular weight; solvent

INTRODUCTION

Despite the large number of articles published over the past decade, the field of electrospinning has not yet reached a stage as a commercially viable option for large scale manufacture of nonwoven fibrous structures. The reason traces back to a lack of fundamental understanding of the complex process mechanisms. Often described as an electrohydrodynamics problem,[1–4] the study of electrospinning requires an understanding of the flow behavior of a viscoelastic polymer solution under an applied electric potential. During the process, a jet of solution ejected from the well-known Taylor cone[5] is subjected to electrical, surface tension, and viscoelastic forces. A dramatic thinning of the jet is achieved through bending, whipping, splitting, and splaying, which are the consequences of electrically induced jet instabilities. Concurrent solidification of the jet alters its mechanical properties during the transit of the solution jet from the Taylor cone to the collector. The physical phenomena associated with solvent evaporation, therefore, add to the complexity in modeling efforts.[3] Difficulty in modeling the flow of polymer solution also arises from a lack of available data related to solution rheology. The complexity of the process is reflected in a number of process parameters that affect the morphology of the final product. A large body of research has identified process parameters that have a significant influence on the morphology of electrospun polymers. However, precise tailoring of the electrospun structure for a specific application requires an understanding of not only the influence of each process parameter but also their cumulative effects.

The structure of electrospun polymer ranges from particulate (in which case the process may also be referred to as ''electrospraying'') to fibers depending on various conditions.[6] In between these extremes, a combination of these morphologies may result in beaded fibers,[7,8] which are often considered as structural defects. As attractive features of electrospinning, these structures may also exhibit wide variations in their shapes and surface morphologies.[9–12] The ultimate goal in electrospinning is to understand how the morphologies of interest are achieved. Some of the recent studies have focused on the transition of these structures, namely the bead-to-fiber transition, with respect to the rheological properties of polymer solutions. McKee et al.[13] and Gupta et al.[14] investigated morphological transitions based on critical hydrodynamic concentrations, i.e., the entanglement concentration (C_e) and the chain overlap concentration (C^*), respectively. Their results indicate that stable fibers start to form for solutions in the semidilute-entangled regime. Shenoy et al.[15] employed a semiempirical approach in establishing a

Correspondence to: S. Shivkumar (shivkuma@wpi.edu).

model for bead-to-fiber transition based on chain entanglement analysis. According to their model, the minimum requirement for the formation of some fibers is one entanglement per polymer chain, whereas more than 2.5 entanglements per chain may be required to form bead-free fibers. The relative comprehensiveness of this model has been indicated by examining the applicability to several polymer–solvent systems.

While the importance of chain entanglements has been recognized, other solution properties are also known to play an important role in determining the morphology of electrospun polymers.[7,16,17] For instance, it is well known that a solution with a high charge density results in a fine fiber structure due to the large extensional force in a jet of solution.[18] Since the solvent used determines solution properties to a large extent, several investigators have explored the change in morphology of polymers electrospun from various solvents.[16–23] Many reports have shown that the use of solvents with a large dielectric constant and electrical conductivity typically results in increased uniformity and reduced number of beads in the electrospun fibers.[19,20,23] The addition of salts[6,7] and surfactants[24] is also known to demonstrate a similar effect. However, a quantitative study of these parameters remains difficult as the effect of solvent properties cannot be isolated. Recently, Larsen et al.[25] were successful in isolating the effect of evaporation rate by the use of a coaxial gas jacket. Their results show that by controlling the evaporation of volatile solvents, bead-to-fiber transitions can be induced. It is implied that the formation of stabilizing junctions within the jet of solution by solvent evaporation plays a vital role in determining the resulting polymer structure. In this case, bead-to-fiber transition is not solely dependent on the entanglement number.

The morphology of electrospun polymer, therefore, may be controlled by various parameters. To predict the resulting structure for a given condition, the contribution of rheological and other effects must be considered. While previous investigations have examined the influence of solution rheology on stable fiber formation for different polymer/solvent systems, the range of molecular weights examined is relatively small and is usually close to the stable fiber formation regime.[10,13–15] In addition, the effects of the solvent on the extent of various regimes for morphological transitions have not been addressed previously. The purpose of this article is to highlight the development of various structures such as beads, beaded fibers, and fibers as a function of polymer molecular weight and solvent properties. The polymer molecular weight has been varied from the values close to the entanglement molecular weight to 3 orders of magnitude above this value. To gain a comprehensive understanding of the morphological transitions, two standard solvents, both with a Mark–Houwink exponent of about 0.7 (i.e., good solvent), but with contrasting nonrheological properties, namely dielectric constant, boiling point, and heat of vaporization, have been used. These data have been utilized to study the applicability of a previously proposed model based on chain entanglement under extreme conditions.[15]

EXPERIMENTAL PROCEDURE

Linear atactic polystyrene (PS) with six different weight average molecular weights (M_w) ranging from 19,300 to 1,877,000 g/mol and a polydispersity index of about 1 was obtained from Scientific Polymer Products (Ontario, NY) and used without further purification. Solutions were prepared by dissolving the polymer in tetrahydrofuran (THF) (Sigma-Aldrich) and *N*,*N*-dimethylformamide (DMF) (Sigma). Both solvents were reagent-grade.

To determine the transition concentration (i.e., bead-to-fiber) for each molecular weight, electrospinning was conducted for several solution concentrations varying in steps of $\sim$ 1–4 times the dilute solution limit for PS in THF (C^*_{THF}), which was calculated according to eq. (1):[26]

$$C^*_{THF} = \frac{1}{[\eta]_{THF}} = \frac{1}{0.011 M_w^{0.725}} \quad (1)$$

where $[\eta]_{THF}$ is the intrinsic viscosity of PS in THF in mL/g, with 0.011 and 0.725 being the corresponding Mark–Houwink constants.[27] The same concentrations were used for the two systems to highlight the effects of the solvent. About 0.5 mL of solution with the desired concentration was prepared and drawn into a 1-mL syringe equipped with an 18-gauge needle (inner diameter = 0.84 mm, 51-mm long). The syringe was placed horizontally on a syringe pump (EW-74900-00, Cole-Parmer), which was calibrated to deliver the solution to the needle tip at a rate of 3 and 1 mL/h for PS-THF and PS-DMF systems, respectively. A grounded aluminum foil collector (10 cm $\times$ 10 cm) was positioned 10 cm from the tip of the needle. In most experiments, a potential of 10 kV was applied to the needle during electrospinning. A limited number of experiments were also conducted at a voltage of 30 kV to highlight the effects of the applied potential on the electrospun morphology. The whole apparatus was enclosed in a Plexiglas box, which was constantly evacuated during the process to control solvent evaporation. The electrospun polymer was dried for at least a day and sputter-coated for scanning electron microscope (JSM-840) examination. Fiber diameter distribution was obtained using a commercial software package, AnalySIS® (Soft Imaging System, CO).

RESULTS AND DISCUSSION

The extent of chain entanglements in the solution can be characterized by various parameters. The critical concentrations such as C^* and C_e are often employed to describe the degree of overlap of hydrodynamic volumes in which the polymer molecules are confined. The limiting concentration for dilute solution, C^*, is determined to some extent by the solvent quality, as the approximate value of C^* can be expressed as the inverse of intrinsic viscosity.[26] Therefore, the value of C^* may be smaller for a good solvent than for a poor solvent. The expression for the entanglement concentration, C_e, for a good solvent is[28]

$$C_e \approx \frac{\rho M_e}{M_w} \tag{2}$$

where ρ is the polymer density and M_e is the entanglement molecular weight of the undiluted polymer. Above C_e, a sharp increase in zero shear viscosity is observed due to extensive chain entanglements. For the PS-THF system, Jamieson and Telford[29] observed this upturn in viscosity to occur for $M_wC_e \sim 3 \times 10^4$. This criteria yields a value of C_e larger than that obtained from eq. (2) by a factor of about two using $\rho = 1.05$ g/cm^3 and $M_e = 16{,}600$ g/mol.[15] McKee et al.[13] showed that, during electrospinning, C_e is the minimum concentration required for the formation of beaded fibers, whereas 2–2.5 times C_e may be required for the formation of bead-free fibers. In a similar manner, Shenoy et al.[15] evaluated the bead-to-fiber transition in terms of the solution entanglement number, $(n_e)_{soln}$, which is a ratio of the polymer molecular weight to its solution entanglement molecular weight, $(M_e)_{soln}$. Using the relationship, $(M_w)_{soln} = M_e/\phi_p$,[28] where ϕ_p is the polymer volume fraction, the solution entanglement number is obtained by calculation from eq. (3):

$$(n_e)_{soln} = \frac{\phi_p M_w}{M_e}. \tag{3}$$

It can be noticed that eqs. (2) and (3) are essentially equivalent for $(n_e)_{soln} = 1$. According to the analysis of Shenoy et al.,[15] the transition in the morphology of electrospun polymer can be predicted by this parameter. The onset of fiber formation, for instance, can be estimated to occur for conditions corresponding to $(n_e)_{soln} = 2$. In terms of C_e, the corresponding concentration is $2C_e$ according to eq. (2), or C_e according to $M_wC_e \sim 3 \times 10^4$. Similarly, complete fibers are expected to form when $(n_e)_{soln} \geq 3.5$.

PS-THF system

During electrospinning, the morphological transition from bead-only to bead-free structure takes place gradually over a range of polymer concentrations. Megelski et al.[10] have shown the transition from bead dominant structure to bead-free fibers for PS with $M_w = 190{,}000$ g/mol electrospun from THF. In this case, the transition was shown to take place for concentrations between 18 and 35 wt %. As has been discussed by Shenoy et al.,[15] these concentrations correspond to $(n_e)_{soln} = 2$ and 3.5, indicating the onset of initial fiber formation and bead-free fiber formation, respectively. Their optical micrographs of the electrospun polymer show that during this transition, the number of beads reduces and the fiber diameter increases with concentration. The general trend of morphological variations observed in the present study was consistent with the results reported to date. SEM photographs of the onset of incipient fiber formation and morphological variation of beads and fibers for $M_w = 393{,}400$ g/mol electrospun from THF are shown in Figure 1. For concentrations well below C_e, which was estimated to be 7.9 wt % (according to $M_wC_e \sim 3 \times 10^4$),[29] the amount of chain entanglement was negligible, and structures consisting only of beads were obtained [Fig. 1(a)]. The types of beads shown in Figure 1 correspond to the range of structures described in our previous work,[12] where a transition from microporous to dish-shaped beads was documented. When the concentration was increased near C_e, incipient fibers emerging from some beads were observed in small fractions [Fig. 1(b)]. Although some isolated beads were observed, the formation of these incipient fibers suggests some degree of chain entanglement in the solution. The solution entanglement number, $(n_e)_{soln}$, calculated for this condition was 1.5, which is in good agreement with the prediction from Shenoy et al.'s model.[15] The fraction of incipient fibers increased with concentration [Fig. 1(c)]. In this regime, the structure of beads varied significantly and the formation of cups with submicron pores was observed. Further increase in concentration resulted in a continuous structure in which all beads were connected by fibers [Fig. 1(d)]. Above this concentration, the occurrence of beads diminished and their shape became more spindle-like [Fig. 1(d,e)] until complete fibers [Fig. 1(f)] were formed. These results are in agreement with the data reported previously.[20] PS fibers electrospun from THF typically had a noncircular cross section [Fig. 1(f)]. The formation of flat fibers was discussed by Koombhongse et al.[9] It is expected that the high evaporation rate of THF may have contributed to skin formation and collapse of the hollow tube, leading to flat fibers. The typical aspect ratio was measured to be 2.4. The ridges and surface undulations observed on some fibers suggest that they may be in the process of splitting.[9] For the PS-THF system, fused structures were typically observed for ex-

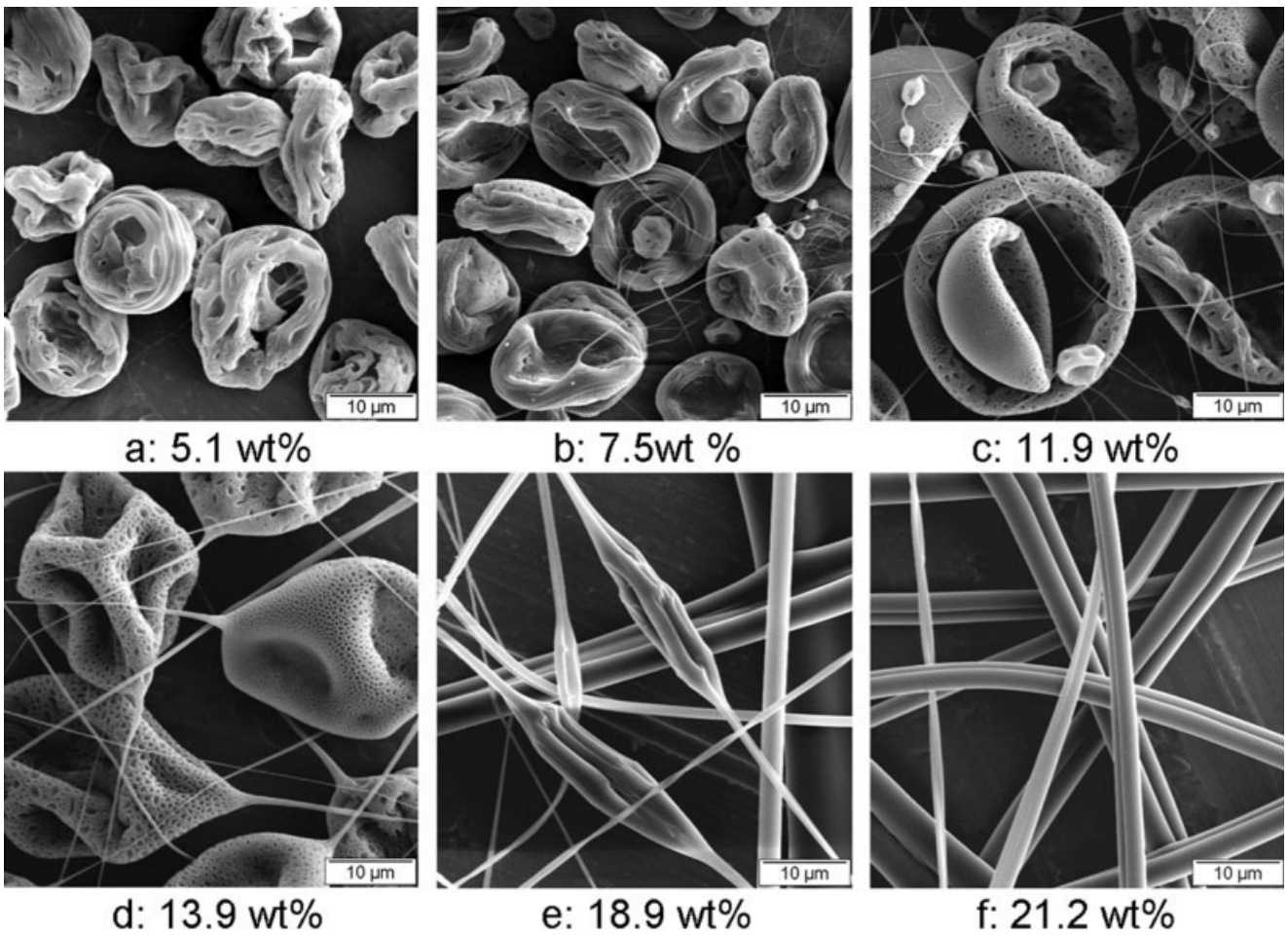

Figure 1 SEM photographs showing different structural regimes during bead-fiber transition. As the concentration is increased, the morphology consists of (a) beads only, (b,c) beads with incipient fibers, (d,e) bead-on-string, and (f) bead-free fibers (M_w = 393,400 g/mol). The corresponding solution concentrations are indicated.

tremely low concentrations ($C < 1$ wt %) as well as for relatively high concentrations at which fibers were produced (Fig. 2). The fiber mat shown in Figure 1(f) also contained some fused fibers at different parts of the sample [Fig. 2(b)], indicating incomplete evaporation of the solvent as the solution jet reached the collector. This observation suggests that two competing factors may contribute to the complete evaporation of the solvent. As the fraction of solvent in the solution is increased, the time it takes for complete evaporation is extended beyond the ''flight time,'' thereby leaving fused structures. On the other hand, as the fraction of solvent is lowered such that only fibers are formed, the effective surface area available for the solvent to evaporate is reduced (as the surface area of fibers is less than that of beads) and complete evaporation is inhibited. It can also be noted that the formation of a skin (often observed for high concentration) may retard solvent evaporation, as the solvent molecules diffuse much more slowly within the skin. Based on these transitions, it can be concluded that for M_w = 393,400 g/mol, the onset of incipient fiber formation occurs at $C = 7.5$ wt % and bead-free fibers are stabilized for $C = 21.2$ wt %. For convenience, these critical concentrations are denoted by C_i and C_f, respectively. Hence, C_i corresponds to the onset of fibers from beads and C_f is the lowest concentration at which a completely fibrous structure is stabilized. Since an increase in concentration results in thicker fibers, C_f may be considered as the lowest concentration at which bead-free fibers with the smallest diameter may be obtained. C_i and C_f are functions of M_w, as can be expected. However, it should also be noted that a change in the electric field strength may shift these values. To illustrate this point, a solution with a concentration slightly below C_i and C_f was electrospun at a voltage of 10 and 30 kV (Fig. 3). Comparing Figures 3(a) and 3(b) (where the same concentration was used), it is apparent that incipient fiber formation is easier at a higher voltage. The underlying mechanism for this phenomenon is not readily evident; however, the rheological properties of the solution may have been altered by the large change in

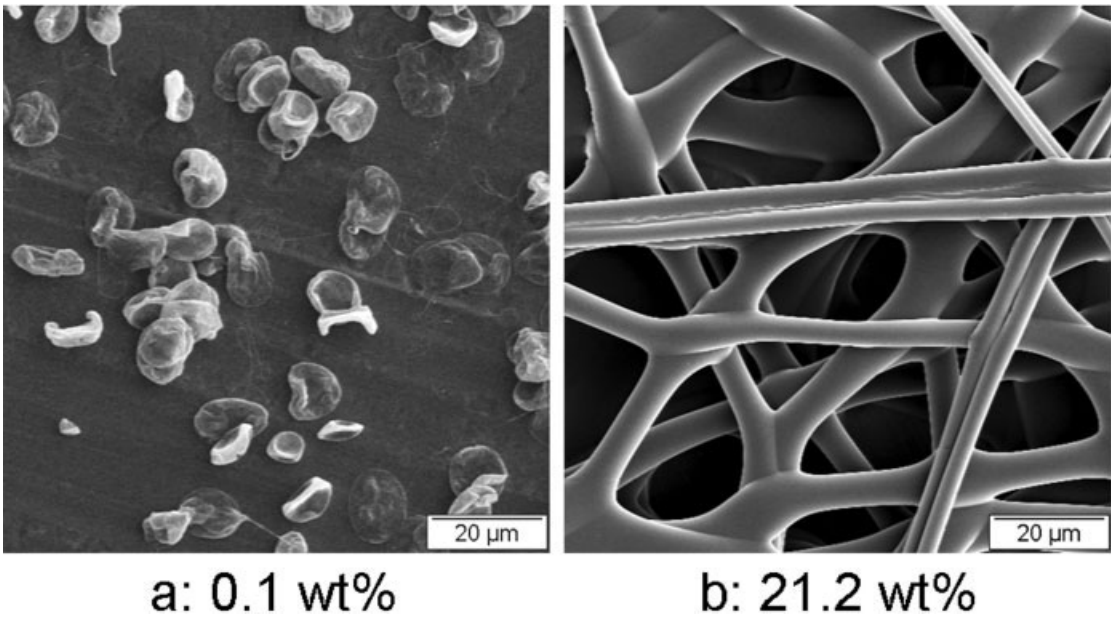

Figure 2 Fused beads and fibers at (a) low and (b) high concentration (M_w = 393,400 g/mol). The corresponding solution concentrations are indicated.

the electric field as previous studies have shown.[30–32] An example of bead elimination from beaded fibers when the voltage is increased is shown in Figure 3(c,d). The absence of beads in Figure 3(d) may be a result of the increased extensional force in the jet induced by increased electric field. Although a large potential may decrease the critical concentrations, too high an electric field is typically not preferred due to defect formation and loss of morphological uniformity.[10] Further examination of the variation of C_i and C_f were conducted at a fixed applied voltage (10 kV).

The reduction in polymer molecular weight significantly increased the concentrations at which morphological transitions took place. For M_w = 19,300 g/mol, a bead-only structure was obtained for concentrations as high as 32.4 wt %, suggesting the lack of chain entanglement in the solution [Fig. 4(a)]. Nevertheless, continuous structures began to form upon increasing the concentration [Fig. 4(b)]. For conditions corresponding to the bead-free fiber formation regime, the calculated $(n_e)_{\text{soln}}$ was less than 1 for low-molecular-weight solutions (19,300, 44,100 g/mol). Although the applicability of Shenoy et al.'s[15] model at these high concentrations may be questioned, the formation of complete fibers with M_w = 19,300 g/mol, which is just above the entanglement molecular weight of 16,600 g/mol,[15] was unexpected. The formation of fibers for low-molecular-weight solutions may be attributed to the rapid solidification of the jet. For concentrated solutions (C > 30 wt %), evaporation of a small amount of solvent may lead to immediate skin formation. It may be speculated that the solution jet ejected from the Taylor cone undergoes solidification, before Rayleigh instability can take effect. In fact, when concentrations higher than 30 wt % were used, the solution solidified immediately after emerging from the capillary and often terminated the electrospinning process in a few seconds. In the beaded-fiber regime, the amount of incipient fibers increased with molecular weight, suggesting enhanced contribution of chain entanglements [Fig. 4(b,e,h)]. However, the fact that complete fibers are observed for $(n_e)_{\text{soln}}$ of 1.7 rather than the predicted value ($\geq$3.5) for M_w = 111,400 g/mol suggests that solvent evaporation may have played a dominant role in jet stabilization.

A bead-to-fiber transition was observed at lower concentrations as the molecular weight is increased. For M_w > 1,000,000 g/mol, a bead-to-fiber transition was observed at C < 12 wt %. Further, when M_w > 1,000,000 g/mol, the bead-only regime was not observed even for the lowest concentration used in this study (0.01 wt %). Some incipient fibers were present even for $C < C^*$ as shown in Figure 5, indicating the presence of chain entanglements in the solution. It is possible that high-molecular-weight polymers were not completely dissolved in the solvent and domains of entangled molecules that remain in the solution may facilitate fiber formation. The variation of bead morphology was similar to the behavior observed with other molecular weights. At concentrations just above C^*, the beads typically had dish-shapes as shown in Figure 5(b). A slight increase in concentration resulted in cup-shaped beads with a smooth surface [Fig. 6(a,d)]. At higher concentra-

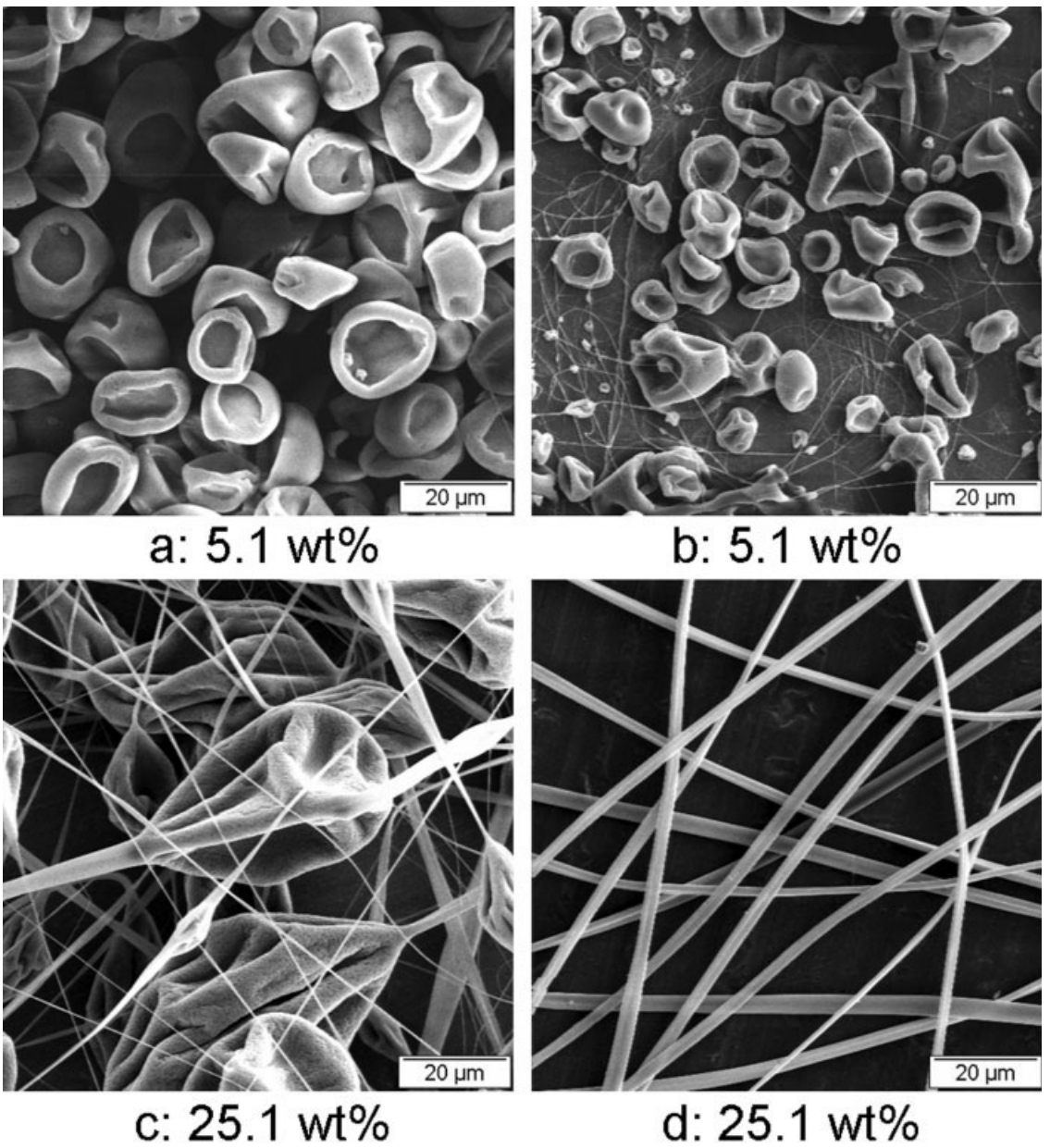

Figure 3 SEM photographs showing the change in bead and fiber morphology with respect to applied voltage. Upon increasing the voltage from 10 kV (a,c) to 30 kV (b,d), fiber formation is facilitated. The corresponding solution concentrations are indicated (M_w = 111,400 g/mol).

tions, spindle-shaped, wrinkled beads were observed [Fig. 6(b,e)]. This transition suggests the formation of a thick and stiff skin at the bead surface induced at high concentrations. The bead-free fibers, obtained with high-molecular-weight polymer, were also flat with an average aspect ratio of about 2.8, which did not vary significantly with molecular weight.

The variation of fiber diameter is generally consistent with previous reports, that is, the fiber diameter increases with C or M_w, when the other parameter is held constant. In this study, the fiber diameter distribution at C_f for different molecular weights was examined (Fig. 7). Note that the fiber distribution shown in Figure 7 corresponds to the lowest concentration at which a bead-free fibrous structure was observed. The average fiber diameter significantly decreased with increasing molecular weight at these concentrations. Further, the distribution shifts toward smaller diameters. This result may be explained by the large difference in the values of $[\eta]$, which is analogous to the size of the hydrodynamic volume. A polymer with large $[\eta]$ defines a large hydrodynamic sphere with extensive coiling. Entanglements are readily formed at a low concentration, and extensional deformation is likely to occur by uncoiling of the chains. The amount of

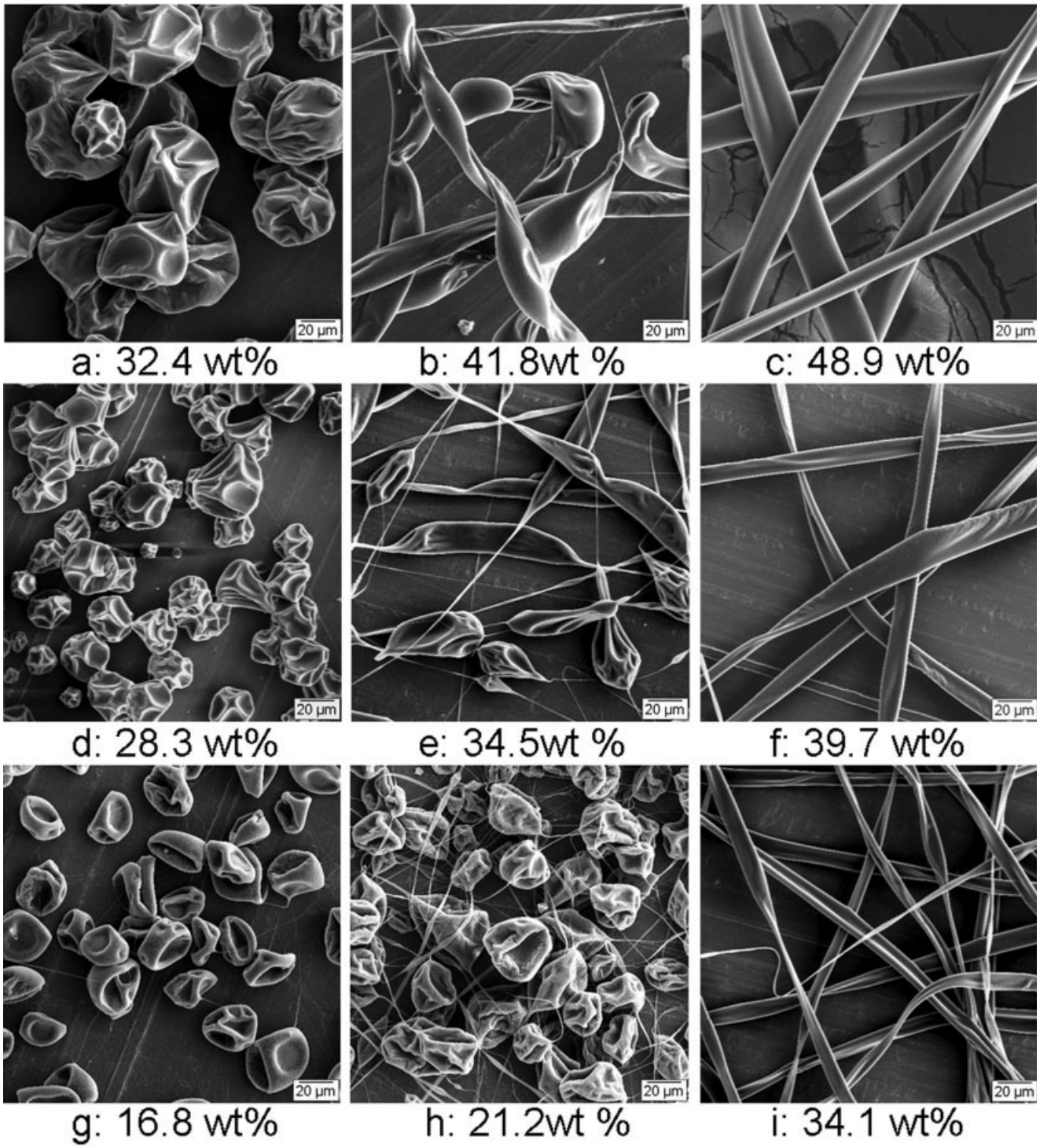

Figure 4 Bead-to-fiber transition observed with low-to-moderate molecular weight PS [(a–c) $M_w = 19{,}300$ g/mol, (d–f) $M_w = 44{,}100$ g/mol, (g–i) $M_w = 111{,}400$ g/mol] electrospun from THF. The corresponding solution concentrations are indicated.

polymer required to stabilize a unit length of fiber may thus be minimal. As a result, if the polymer concentration is optimized, the fiber diameter may be smaller for high-molecular-weight polymers. The multimodal fiber distribution reported previously by many investigators[33,34] was also observed in this study.

PS-DMF system

DMF is a moderately good solvent for PS, with Mark–Houwink constants $K = 31.8$ mL/g and $a = 0.603$.[27] The use of DMF in electrospinning has been reported by many investigators.[16–21] DMF is a polyelectrolytic solvent with relatively high dielectric constant (36.4)

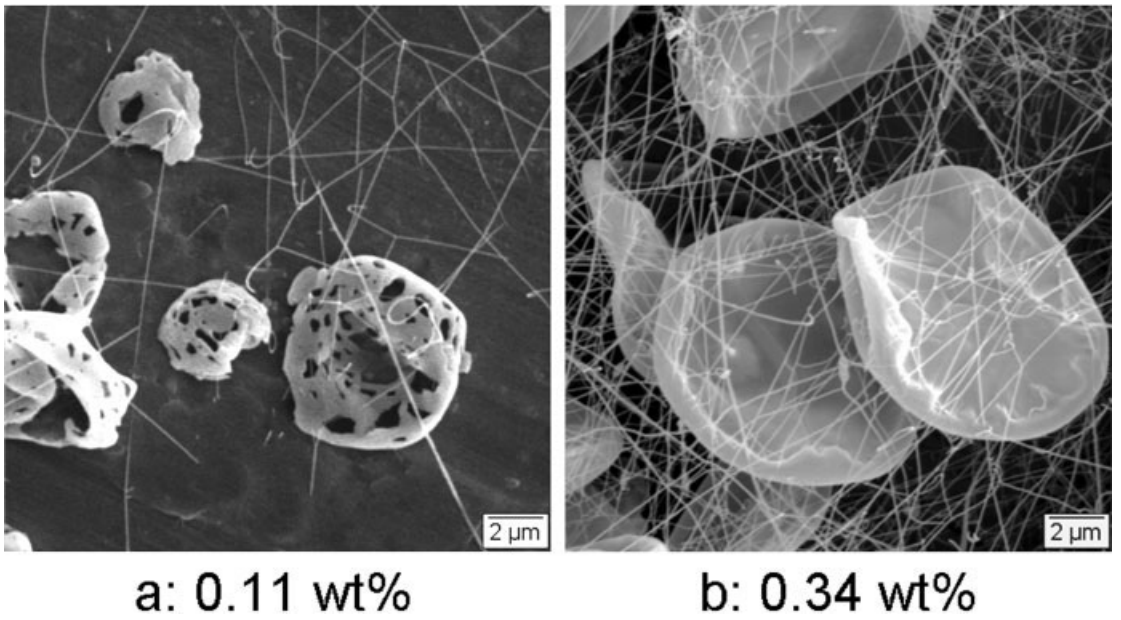

Figure 5 Incipient fibers forming at extremely low concentrations for M_w = 1,877,000 g/mol [(a) C = 0.11 wt %, (b) C = 0.34 wt %].

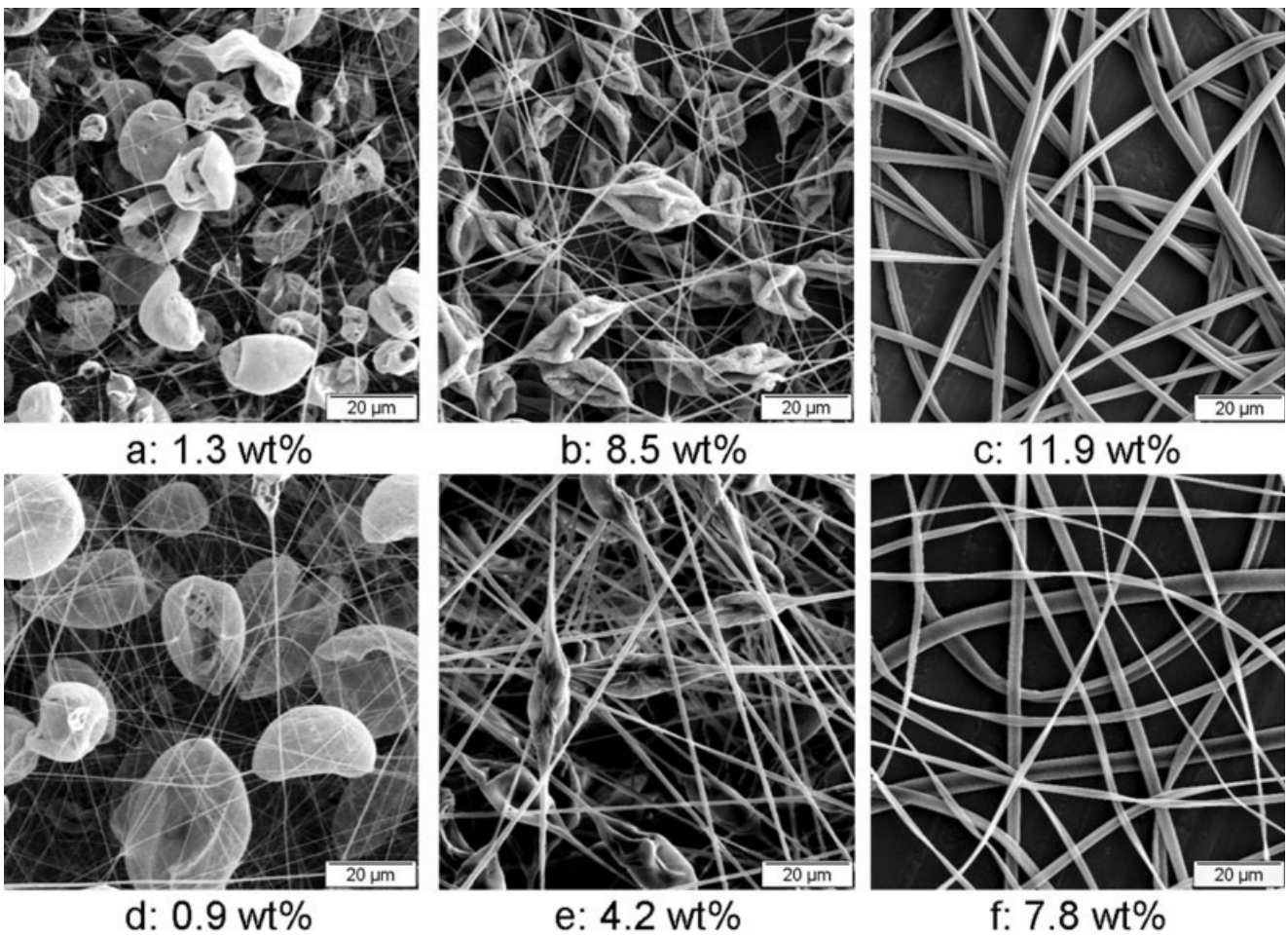

Figure 6 Change in the morphology of high-molecular-weight PS [(a–c) 1,045,000 g/mol, (d–f) 1,877,000 g/mol] electrospun from THF. The corresponding solution concentrations are indicated.

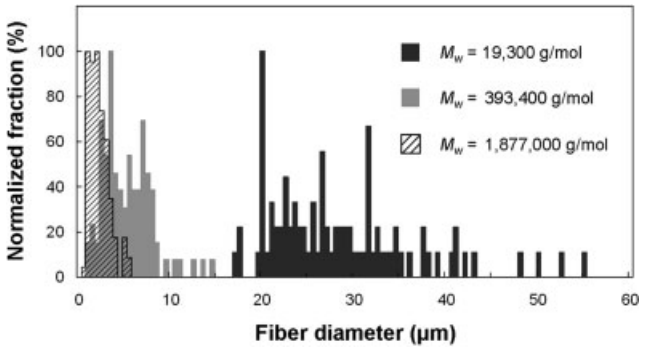

Figure 7 Fiber diameter distribution as a function of polymer molecular weight (M_w) at the critical concentration, C_f, at which bead-free fibers are observed for PS-THF system.

compared to that of THF (7.6). The primary effect of using DMF instead of other electrically ''poor'' solvents is the reduction in fiber diameter due to increased elongational force within the solution jet. Lee et al.[20] observed the reduction of beads at a condition in the beaded fiber regime when DMF was used in place of THF during electrospinning of PS. One of the principal observations from this study which showed a reduction in fiber diameter and bead formation with a change in solvent from THF to DMF was in general agreement with several previous reports.[19–21] The bead-to-fiber transition for M_w = 393,400 g/mol is shown in Figure 8. At C = 2.5 wt %, the electrospun structure consisted of beads only [Fig. 8(a)]. The beads obtained at this condition formed a rough surface that was unlike any of those observed with the PS-THF system. This type of surface was typically observed for solutions with low concentrations (<5 wt %). Upon increasing the concentration, an incipient fiber regime was observed [Fig. 8(b)]. Compared to the data for the PS-THF system, the fraction of incipient fibers is high at this stage. A further increase in concentration resulted in the formation of beaded and bead-free fibers [Fig. 8(c,d)]. The critical concentrations, C_i and C_f, for M_w = 393,400 g/mol in PS-DMF system were determined to be 4.8 and 20.2 wt %, respectively. In comparison with the data for THF as the solvent, C_i and C_f are very similar. Considering the fact that DMF is not as good a solvent for PS as THF, it may be assumed that the difference in solvent quality exhibited between THF and DMF may not have a significant effect on the morphological transitions for this molecular weight. The fact that the values of C_f obtained from two systems were similar was also unexpected, as DMF is known to reduce the fraction of beads[20] as mentioned earlier. In fact, in most cases, the number and the size of beads on the fibers were reduced. However, complete removal of beads from the fibers required concentrations comparable to C_f in the PS-THF system.

The variations in bead and fiber morphology were limited when DMF was used as the solvent (Fig. 9), unlike the case with the PS-THF system. Typically, the beads obtained with DMF for $C < C_i$ were nearly spherical and formed a smooth surface unlike the wrinkles observed with THF. This may be the result of the low evaporation rate of DMF. THF having lower boiling point and heat of vaporization compared to DMF is expected to evaporate at a much slower rate. Immediate evaporation of the solvent may induce skin formation and collapse, which results in the shape variation of beads and fibers. Despite the large difference in evaporation rate between the two solvents, fused structures (indicative of incomplete solvent evaporation), which were often observed with the PS-THF system, were rarely observed in the PS-DMF system. This result may be attributed to the fine structures obtained with DMF as the solvent. By comparing Figures 4 and 9, for example, it can be noticed that beads and fibers obtained with DMF as the solvent are almost an order of magnitude smaller than those produced with THF.

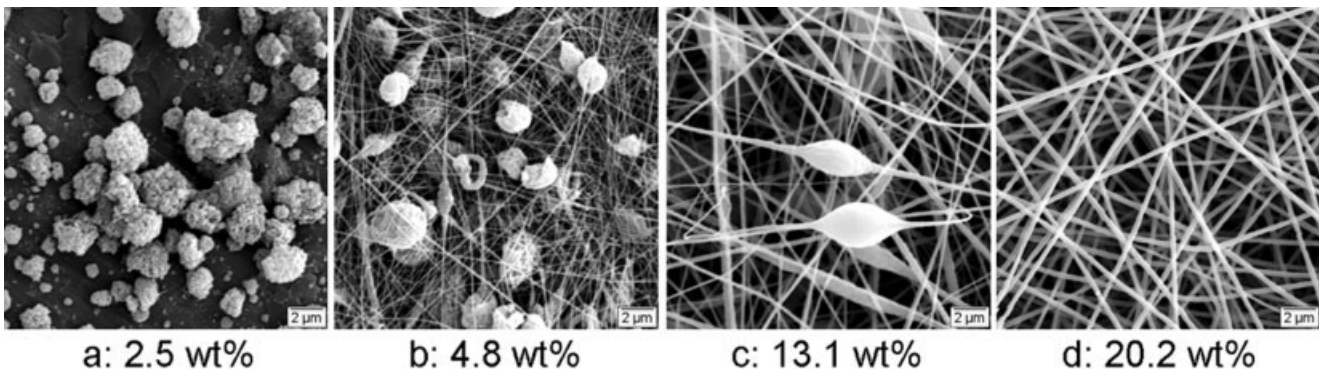

Figure 8 Different structural regimes during bead-fiber transition of PS electrospun from DMF. As the concentration is increased, the morphology consists of (a) beads only, (b) beads with incipient fibers, (c) bead-on-string, and (d) bead-free fibers. The corresponding solution concentrations are indicated.

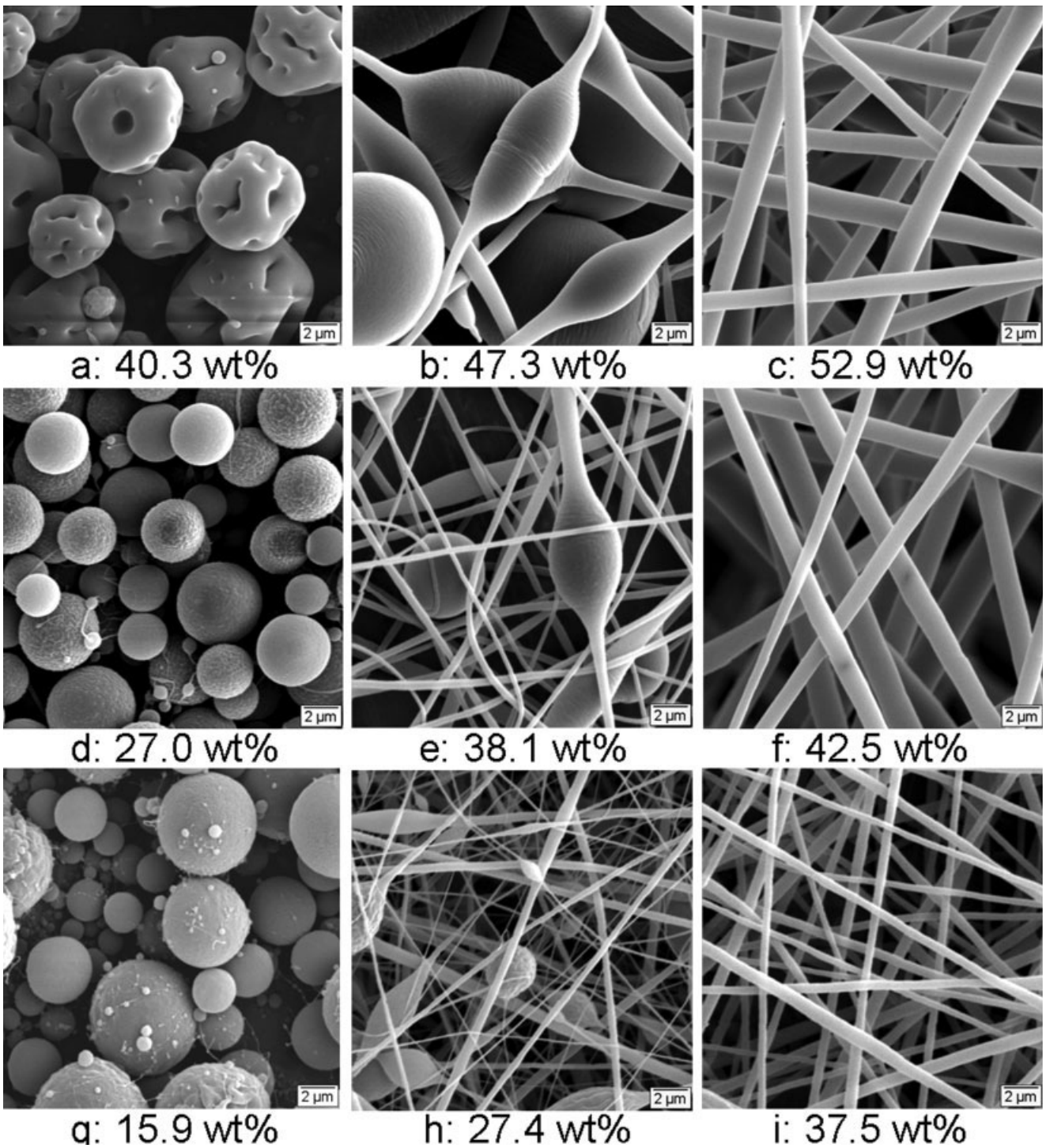

Figure 9 Bead-to-fiber transition observed with low-to-moderate molecular weight PS [(a–c) 19,300 g/mol, (d–f) 44,100 g/mol, (g–i) 111,400 g/mol] electrospun from DMF. The corresponding solution concentrations are indicated.

Therefore, the total area from which the solvent can evaporate should be an order of magnitude larger.

The increase in C_i and C_f with decreasing molecular weight was similar to that of the PS-THF system; however, the transitions did not occur at the same concentrations. For M_w = 19,300 g/mol, a bead-only structure was observed for concentrations up to 40 wt % [Fig. 9(a)]. It may be recalled that at this concentration, some fibers may start to form for the PS-THF system [Fig. 4(b)]. Beaded fibers for this molecular weight were observed for C = 47.3 wt %, at which concentration bead-free fibers could be seen with THF [Fig. 4(c)]. In other words, at this molecular weight and concentration, the use of DMF promoted

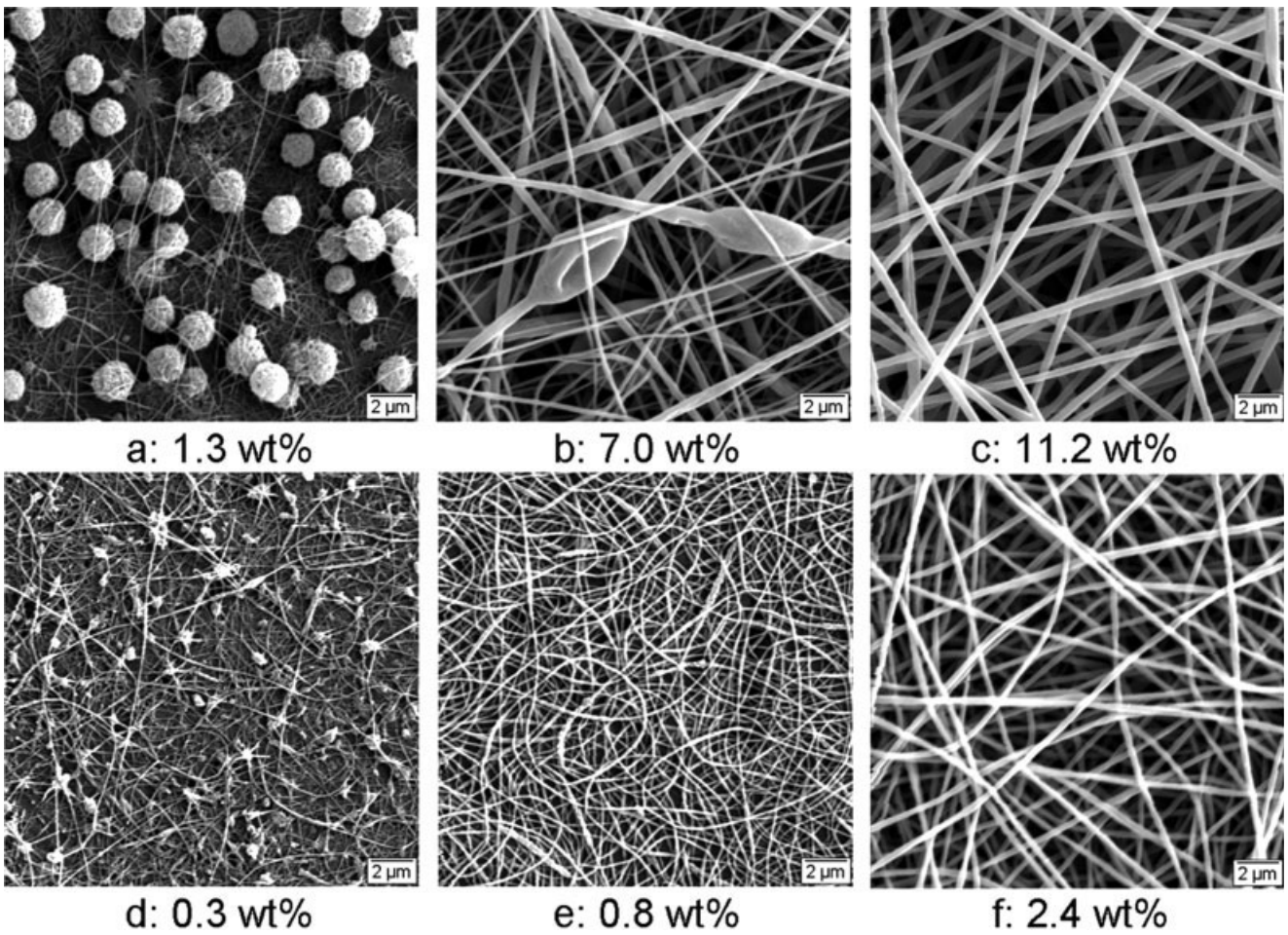

Figure 10 Change in the morphology of high-molecular-weight PS [(a–c) 1,045,000 g/mol, (d–f) 1,877,000 g/mol] electrospun from DMF. The corresponding solution concentrations are indicated.

the formation of beads rather than suppressing their presence. This behavior may again be attributed to the difference in evaporation between the two solvents. When DMF is used as the solvent, complete solidification takes place after Rayleigh instability develops. In this concentration regime where solidification is rapid, the effect of high charge density in removing beads may be minimal.

High-molecular-weight solutions (M_w = 1,045,000; 1,877,000 g/mol) resulted in structures containing some fibers for all concentrations examined (Fig. 10). For M_w = 1,045,000 g/mol, the transition from beaded to bead-free fibers occurred at C = 11.2 wt %, which was essentially the same the value as obtained for PS-THF system. For M_w = 1,877,000 g/mol, however, bead-free fibers were obtained for concentration as low as 0.8 wt %, which is significantly lower than values of C_f obtained for other conditions. The normalized critical concentration, C_f/C^*, for M_w = 1,877,000 g/mol, is about 1.5, whereas the corresponding value is calculated to be above 12 for all other conditions. The reason for this sudden drop of C_f with respect to molecular weight is not readily evident; however, the large difference in C_f/C^* suggests that the mechanisms involved in yielding bead-free fibers may have been different in this particular case. The fiber diameter distribution of PS-DMF systems at C_f is shown in Figure 11. At C_f, an increase in molecular weight significantly

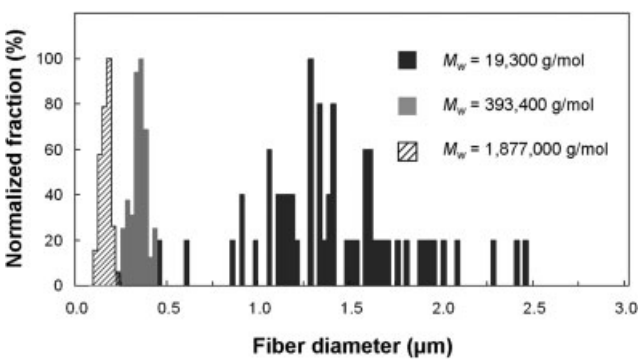

Figure 11 Fiber diameter distribution as a function of polymer molecular weight (M_w) at the critical concentration, C_f, at which bead-free fibers are observed for PS-DMF system.

reduced the fiber diameter and shifted the overall distribution to smaller diameters, similar to the results with the PS-THF system. The use of DMF as the solvent typically resulted in unimodal fiber distribution. This result is consistent with previous reports on the fiber distribution in other electrospun polymers.[19,21]

The variation of C_i and C_f as a function of molecular weight for both solvents is shown in Figure 12. For high molecular weights where bead-only structure was not observed, the lowest concentration examined in this study was taken as C_i. Relevant data from previous reports[10,20] are also shown for comparison. The predicted transition concentration for PS-THF system based on the solution entanglement number model[15] is indicated. It is apparent that the deviation from the prediction is significant for molecular weights below 100,000 g/mol. As mentioned earlier, for these molecular weights, fiber formation may be facilitated possibly due to the rapid solidification of the jet owing to high polymer concentrations. The difference in the values of C_i and C_f for the two systems is minimal for most cases. At low-to-moderate values of M_w ($\leq$111,400 g/mol), C_i and C_f are slightly larger for the PS-DMF system than for the PS-THF system, suggesting that fiber stabilization may have been impeded by the low evaporation rate of DMF.

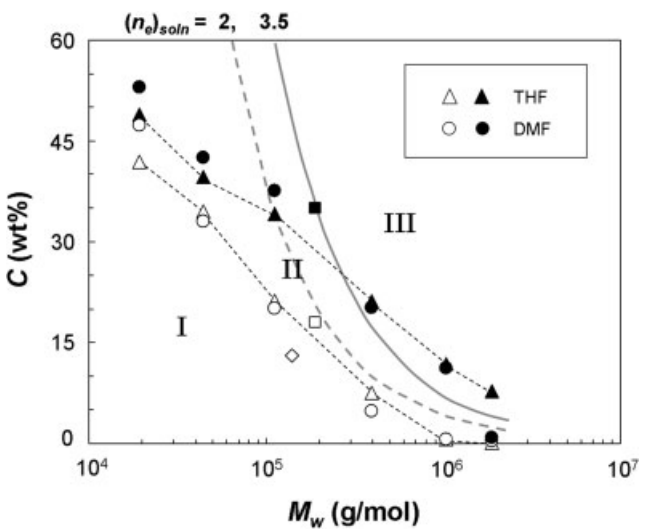

Figure 12 Variation of C_i and C_f as a function of molecular weight for PS-THF and PS-DMF systems. The regions I, II, and III indicate the conditions at which beads only, beaded fibers, and bead-free fibers were observed, respectively. The transition concentrations predicted from the solution entanglement number model[15] is plotted for comparison. The dashed and solid lines in gray indicate conditions corresponding to $(n_e)_{soln}$ = 2 and 3.5, respectively. The data of Megelski et al. (□, ■)[10] and Lee et al. (◇)[20] are also shown. □ and ◇ indicate the conditions at which bead-dominant morphologies are observed, whereas ■ corresponds to a condition at which bead-free fibers are observed.

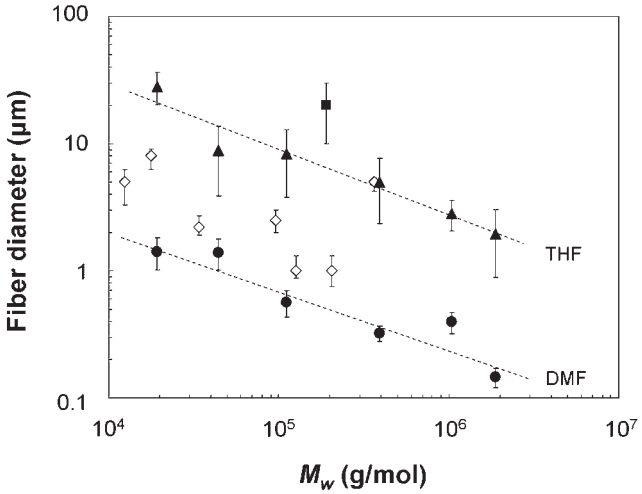

Figure 13 Average fiber diameter as a function of molecular weight for PS-THF and PS-DMF systems at the critical concentration, C_f, at which bead-free fibers are observed. The data of Megelski et al.[10] is indicated as a solid square (■). Relevant data of Gupta et al.,[14] who examined PMMA-DMF system, are shown as open diamond (◇) for comparison.

Fiber diameter

Extensive theoretical and experimental analysis has shown that the fiber diameter depends on both molecular weight and concentration. It has been shown that fiber diameter may be correlated with critical concentrations, C^* and C_e.[13,14] In this study, a different approach was taken to evaluate the effect of molecular weight. The variation of fiber diameter as a function of molecular weight for $C = C_f$ is shown in Figure 13. The fiber distribution is plotted at the minimum concentration at which bead-free fibers were observed. At this condition, the average fiber diameter decreases consistently with molecular weight for both systems. Interestingly, for both systems, the fiber diameter obeys a power law relationship with molecular weight, with an exponent of -0.5. This result suggests that the effect of molecular weight may be independent of solvent properties. A similar tendency is observed in the results of Gupta et al.,[14] who examined PMMA-DMF system for a range of molecular weights. Relevant results selected from their work are plotted in Figure 13 for comparison. The data of Megelski et al.[10] (also shown in Fig. 13) diverge slightly from the results obtained in this study, perhaps due to different processing conditions, such as applied electric field and working distance.

CONCLUSIONS

The morphology of electrospun PS depends significantly on polymer molecular weight, concentration, and solvent. The morphological transitions from

bead-dominant structure to bead-free fibers can be characterized by two critical concentrations, C_i and C_f. These values decrease considerably with increasing molecular weight due to the chain entanglement effect. The applied voltage may also influence the transition. The solvent has minimal effect on the critical concentrations for $M_w > 100{,}000$ g/mol. The transition concentrations are generally consistent with the prediction of entanglement model proposed by Shenoy et al.[15] for $M_w > 100{,}000$ g/mol. However, for $M_w < 100{,}000$ g/mol, fibrous structures may be obtained at concentrations appreciably lower than those predicted by their model. For solutions with high concentration ($C > 30$ wt %), fibers may be partially stabilized through rapid jet solidification during the initial stages. The use of a volatile solvent may facilitate fiber formation.

The morphology of beads and fibers varies noticeably with the PS-THF system, perhaps owing to the rapid evaporation of the solvent. Fibers electrospun from THF are typically flat and have diameters an order of magnitude larger than those obtained with DMF. The average fiber diameter decreases significantly with molecular weight for conditions corresponding $C = C_f$, which is the minimum concentration for bead-free fiber formation. At this condition, the average fiber diameter may be considered as the minimum for a given molecular weight and the accompanying process conditions. The average fiber diameter for $C = C_f$ was found to be proportional to $M_w^{-0.5}$ regardless of the solvent.

References

1. Reneker, D. H.; Yarin, A. L.; Fong, H.; Koombhongse, S. J Appl Phys 2000, 87, 4531.
2. Hohman, M. M.; Shin, M.; Rutledge, G.; Brenner, M. P. Phys Fluids 2001, 13, 2201.
3. Yarin, A. L.; Koombhongse, S.; Reneker, D. H. J Appl Phys 2001, 89, 18.
4. Feng, J. J. J Non-Newtonian Fluid Mech 2003, 116, 55.
5. Taylor, G. I. Proc Roy Soc Lond A 1969, 313, 453.
6. Zong, X.; Kim, K.; Fang, D.; Ran, S.; Hsiao, B. S.; Chu, B. Polymer 2002, 43, 4403.
7. Fong, H.; Chun, I.; Reneker, D. H. Polymer 1999, 40, 4585.
8. Zuo, W.; Zhu, M.; Yang, W.; Yu, H.; Chen, Y.; Zhang, Y. Polym Eng Sci 2005, 45, 704.
9. Koombhongse, S.; Liu, W.; Reneker, D. H. J Polym Sci Part B: Polym Phys 2001, 39, 2598.
10. Megelski, S.; Stephens, J. S.; Rabolt, J. F.; Chase, D. B. Macromolecules 2002, 35, 8456.
11. Liu, J.; Kumar, S. Polymer 2005, 46, 3211.
12. Eda, G.; Shivkumar, S. J Mater Sci 2006, 41, 5704.
13. McKee, M. G.; Wilkes, G. L.; Colby, R. H.; Long, T. E. Macromolecules 2004, 37, 1760.
14. Gupta, P.; Elkins, C.; Long, T. E.; Wilkes, G. L. Polymer 2005, 46, 4799.
15. Shenoy, S. L.; Bates, W. D.; Frisch, H. L.; Wnek, G. E. Polymer 2005, 46, 3372.
16. Lee, K. H.; Kim, H. Y.; Khil, M. S.; Ra, Y. M.; Lee, D. R. Polymer 2003, 44, 1287.
17. Son, W. K.; Youk, J. H.; Lee, T. S.; Park, W. H. Polymer 2004, 45, 2959.
18. Yang, Q.; Zhenyu, L. I.; Hong, Y.; Zhao, Y.; Qiu, S.; Wang, C. E.; Wei, Y. J Polym Sci Part B: Polym Phys 2004, 42, 3721.
19. Lee, K. H.; Kim, H. Y.; La, Y. M.; Lee, D. R.; Sung, N. H. J Polym Sci Part B: Polym Phys 2002, 40, 2259.
20. Lee, K. H.; Kim, H. Y.; Bang, H. J.; Jung, Y. H.; Lee, S. G. Polymer 2003, 44, 4029.
21. Hsu, C. M.; Shivkumar, S. Macromol Mater Eng 2004, 289, 334.
22. Wu, X.; Wang, L.; Yu, H.; Huang, Y. J Appl Polym Sci 2005, 97, 1292.
23. Eda, G.; Liu, J.; Shivkumar, S. Eur Polym, to appear.
24. Lin, T.; Wang, H.; Wang, X. Nanotechnology 2004, 15, 1375.
25. Larsen, G.; Spretz, R.; Velarde-Ortiz, R. Adv Mater 2004, 16, 166.
26. Graessley, W. W. Polymeric Liquids and Networks: Structure and Properties; Garland Science: New York, 2004.
27. Brandrup, J.; Immergut, E. H.; Grulke, E. A. Polymer Handbook, 4th ed.; Wiley: New York, 1999.
28. Ferry, J. D. Viscoelastic Properties of Polymers, 3rd ed.; Wiley: New York, 1980.
29. Jamieson, A. M.; Telford, D. Macromolecules 1982, 15, 1329.
30. Price, C.; Deng, N.; Lloyd, F. R.; Li, H.; Booth, C. J Chem Soc Faraday Trans 1995, 91, 1357.
31. Wang, C. H.; Huang, Q. R. J Chem Phys 1997, 106, 2819.
32. Sun, Z.; Wang, C. H. Macromolecules 1999, 32, 2605.
33. Deitzel, J. M.; Kleinmeyer, J.; Harris, D.; Tan, N. C. B. Polymer 2001, 42, 261.
34. Hsu, C.-M.; Shivkumar, S. J Mater Sci 2004, 39, 3003.